Desalination and Water Treatment
www.deswater.com

doi:10.5004/dwt.2018.22742

124 (2018) 267–278
August

Competitive adsorption of selenite [Se(IV)], selenate [Se(VI)] and selenocyanate [$SeCN^-$] species onto TiO_2: Experimental findings and surface complexation modelling

Bashir Alhaji Labaran, Muhammad Shariq Vohra*

Civil and Environmental Engineering Department, King Fahd University of Petroleum and Minerals (KFUPM), Dhahran31261, Saudi Arabia, email: labaran@uohb.edu.sa (B.A. Labaran), Tel. +966-013-860-2854, Fax +966-013-860-2879, email: vohra@kfupm.edu.sa (M.S. Vohra)

Received 1 December 2017; Accepted 9 July 2018

ABSTRACT

Competitive adsorption of aqueous Se(IV) (selenite), Se(VI) (selenate) and $SeCN^-$(selenocyanate) species onto titanium dioxide/TiO_2 was investigated under a varying set of mixed binary and tertiary systems. The obtained anionic type adsorption curves for binary Se(IV)/Se(VI) systems indicated that Se(IV) adsorption is not affected by Se(VI) species however Se(VI) adsorption is markedly suppressed in presence of Se(IV). This was explained based on higher relative affinity of TiO_2 surface sites for Se(IV) compared to Se(VI). The Se(VI) species showed a sharp anionic type adsorption curve between pH 2–5 whereas Se(IV) adsorption gradually decreased from pH 2–4 followed by a sharp decrease till pH 7. Unlike the Se(IV)/Se(VI) results the binary Se(IV)/$SeCN^-$ and Se(VI)/$SeCN^-$ systems did not show competitive adsorption behavior. Furthermore the tertiary systems having mixed Se(IV), Se(VI), and $SeCN^-$ species showed adsorption trends that were similar to above noted binary systems observations. The respective studies indicated the following adsorption trend above pH 4: Se(IV) > $SeCN^-$ > Se(VI). Adsorption modelling using the *Diffuse Layer Model* also showed reasonable predictions. For Se(IV) an inner sphere Ti-SeO_3^- complex generally yielded acceptable modelling estimations whereas for Se(VI) and $SeCN^-$ outer sphere complexes Ti-H_2O-SeO_4^- and Ti-H_2O-SeCN- respectively showed reasonable modelling results.

Keywords: TiO_2; Adsorption; Selenite-Se(IV); Selenate-Se(VI); Selenocyanate-$SeCN^-$

1. Introduction

Aqueous streams and discharges from sources such as agricultural fields [1], mining areas [1–4], fossil fuel [5] and several other specific industries introduce selenium species in to the environment. The dominant selenium species in industrial effluents is in Se(VI) form whereas under reducing conditions Se(IV)species is also present. Furthermore $SeCN^-$ is another dominant species specifically in petroleum refineries, and fossil fuels based powerplants [6].

Selenium despite being an essential micronutrient, poses adverse effects at higher intake levels [7–15]. Therefore, very stringent selenium drinking water and wastewater treatment standards are in force for which various treatment methods have been employed including TiO_2-photocatalysis [16–19], biological treatment [20], phytoremediation [21], electrocoagulation [22], chemical reduction [23], and adsorption [24]. The use of adsorption process has been widely reported for the removal of various aqueous phase pollutants [25–29].

Though various studies have also explored the adsorption of selenium species onto different materials including iron oxides [30], montmorillonites [31], chitosan–clay composites and ironoxides [8], aluminum oxide [32], etc., investigations on selenium species adsorption onto TiO_2 are limited [7,24,33–41], with only few detailed selenium adsorption work onto TiO_2 [24]. Furthermore, there is no work on com-

*Corresponding author.

petitive adsorption of Se(IV), Se(VI) and $SeCN^-$ species onto TiO_2 surface. As synergistic effects might affect the adsorption of Se(IV), Se(VI) and $SeCN^-$ onto TiO_2 in mixed binary or tertiary competitive adsorption systems, understanding such competitive adsorption behavior is important to realize its role during TiO_2-photocatalysis [42–45]. For example, adsorption of selenium species onto metal oxides is noted to be affected by the presence of other anionic species such as phosphate [46,47], sulphate [47], chromate [48], molybdate [48], silicate [49], fluoride [49], citrate, oxalate, and carbonate/bicarbonate [50] due to differences in strength and type of bonding between the anions and the metal oxide surface and also the binding rate on the surface [48]. Hence studying the competitive adsorption behavior of respective selenium species (i.e., Se(IV), Se(VI) and $SeCN^-$) onto $TiO_2$is also important to better understand the adsorption trends under both binary and tertiary system conditions.

As mentioned above that the application of TiO_2-assisted photocatalysis has been reported for the removal of several Se-based species, and hence it would be very interesting to understand how such species (i.e., Se(IV), Se(VI) and $SeCN^-$) adsorb onto TiO_2 under both binary and tertiary conditions. Such an understanding will help to design better TiO_2 based adsorption and photocatalysis systems for the removal of Se(IV), Se(VI) and $SeCN^-$ species. Considering this, the present study focused on competitive adsorption of Se(IV), Se(VI) and $SeCN^-$ species onto TiO_2 surface. Furthermore considering the importance of specialized surface complexation models such as the Diffuse Layer Model (DLM) for adsorption modelling [51–53] an extensive modelling study was also completed. Details on both experimental and modelling results are reported in the following sections.

2. Materials and methods

2.1. Materials

All chemicals used were of high purity reagent grade quality. The main chemicals included sodium selenite (Aldrich, USA), potassium selenate (Aldrich, USA), potassium selenocyanate (Aldrich, USA), sodium carbonate (BDH, U.K.), sodium bicarbonate (BDH, U.K.), and pH calibration standards (Fisher, USA). The DEGUSSA P25 titanium dioxide/TiO_2 (Degussa, Germany) was used for all adsorption studies. The respective TiO_2 was used as is, without any purification or modification. Table 1 provides several physico-chemical properties of Degussa P25 TiO_2. The pH adjustments were made using either HCl (Surechem, UK) or NaOH (J.T. Baker, U.S.A) solutions. All glassware used were Pyrex based that were appropriately cleaned, washed, and dried before each use. All sample collection, storage, and processing accessories were also cleaned, washed, and dried before each use.

2.1.1. Adsorption experimental details

Stock solutions (1000 ppm) for Se(IV)/SeO_3^{2-}, Se(VI)/SeO_4^{2-}, and $SeCN^-$ were prepared using above mentioned reagent grade chemicals and high purity de-ionized water (Corning Mega Pure™ System), and stored in Pyrex bottles under dark conditions. For the adsorption experiments, the respective selenium-species solutions were prepared using the above-mentioned stock solutions and de-ionized water. A blank sample was first collected after which 1 g/L TiO_2 was added with appropriate mixing to ensure its complete dispersion. This suspension was then transferred to a set of Pyrex glass bottles. Each experiment was conducted in a set of nine bottles by adjusting the pH of the suspensions between 2 and 11 using HCl and/or NaOH solutions. The test solutions were vigorously mixed for about 24 h and the final suspension pH was measured before sample collection and filtration using 0.2-µm membrane filters (WHATMAN, Germany). The syringe and filter holders were also appropriately washed and dried before each use. The collected samples were then duly stored before being analyzed for the target selenium species.

Table 1
TiO_2 parameters used in the Diffuse Layer Model

Parameter	Value
Specific surface area (m^2/g)	55
Surface site density (mmol/g)	0.274
Solid concentration (g/L)	1
pH_{zpc}	6.5
Primary particle size (nm)	30
Crystal phase ratio	75–80% Anatase, 20–25% Rutile

2.1.2. Analytical methods

The filtered sample aliquots were analyzed for Se(IV), Se(VI), and $SeCN^-$ using an advanced ion chromatograph set-up (Metrohm, Switzerland) equipped with conductivity detector. The eluent composition was 2.7 mM Na_2CO_3/3.0 mM $NaHCO_3$and column used was anion Dual 2 IC column (6.1006.100, 4.6 mm × 75 mm, Metrohm, Switzerland). Total selenium was analyzed using an atomic absorption spectrophotometer setup (Perkin Elmer, U.S.A) that was equipped with both flame and furnace units. A standard ICP setup (Thermo, U.S.A) was also utilized for total selenium analysis. The solution pH was analyzed using a standard pH electrode-meter setup (AccuTupH$^+$ 13-620-185 electrode, Accumet XL15 pH meter, Singapore). The XPS analyses were completed by the XPS lab at the physics department of KFUPM. Also, all analytical instruments were regularly calibrated.

2.1.3. Modelling approach

Visual MINTEQ version 3.1 was employed for all surface complexation modelling (SCM) exercises. Its extensive database can support the speciation, solubility, and adsorption modelling of many aqueous species of interest. The TiO_2 surface complexation reactions employed for modelling are shown in Table 2 [52–53]. Also the *Diffuse Layer Model* (DLM) incorporated into MINTEQ software was selected for surface complexation modelling. Furthermore the current version of Visual MINTEQ does not have selenocyanate ($SeCN^-$) in its database. However,

Table 2
Surface complexation reactions employed for adsorption modeling

S/No.	Reaction	Log K_{int}^{s}
1	$\underline{Ti}OH + H^+ \rightleftarrows \underline{Ti}OH_2^+$	3.9[a]
2	$\underline{Ti}OH \rightleftarrows \underline{Ti}O^- + H^+$	–8.7[a]
3	$\underline{Ti}OH + HSeO_3^- \rightleftarrows \underline{Ti}SeO_3^- + H_2O$	4.6[b]
4	$\underline{Ti}OH + SeO_4^{2-} + H^+ \rightleftarrows \underline{Ti} - H_2O - SeO_4^-$	4.8[b]
5	$\underline{Ti}OH + SeCN^- + H^+ \rightleftarrows \underline{Ti} - H_2O - SeCN$	6.55[b]

[a][52]
[b][53]

Table 3
Important aqueous speciation reactions employed for adsorption modelling

S/No.	Reaction	Log K
1	$CN^- + H^+ \leftrightarrow HCN$	9.21[c]
2	$SeCN^- + H^+ \leftrightarrow HSeCN$	–3.77[d]
3	$SeO_4^{2-} + H^+ \leftrightarrow HSeO_4^-$	1.7[c]
4	$HSeO_3^- \leftrightarrow SeO_3^{2-} + H^+$	–8.4[c]
5	$HSeO_3^- + H^+ \leftrightarrow H_2SeO_3$	2.63[c]
6	$OH^- + H^+ \leftrightarrow H_2O$	–13.997[c]

[c]VisualMinteq Database
[d]From Chemicalize.org

the Visual MINTEQ allows for specific changes to its database and thus $SeCN^-$ and HSeCN species were added to the database as component and species, respectively (Table 3). Some other aqueous speciation reactions from MINTEQA2 database are also presented in Table 3. Also Figs. 1a–c provide the speciation diagrams (completed using MINTEQ) for TiO_2, Se(IV), and Se(VI) species; these will be recalled later to elucidate some of the experimental findings.

3. Results and discussion

3.1. Binary systems

The adsorption of respective selenium species onto TiO_2 was first studied at varying pH and binary solution matrices. The respective experimental and modelling results are discussed in this section. Figs. 2a–d provides adsorption results for the binary Se(IV)/Se(VI) systems. Fig. 2a shows the effect of Se(VI) onto adsorption of Se(IV). In the absence of Se(VI), about 89% Se(IV) adsorption transpires at pH 2, which first gradually decreases to 65% till pH 4 and then onwards sharply to 31% till pH 7. The TiO_2 surface speciation (Fig. 1a) shows that Ti-OH_2^+ is the dominant surface species below pH 3.9 and thus interaction between the cationic TiO_2 surface and anionic $HSeO_3^-$ species which is dominant above pH 2.63 yields higher Se(IV) adsorption between pH 2 and 4 (Fig. 2a and Scheme 1). However, with an increase in pH to 4, theTi-OH_2^+surface species reduces to 50% and then to a very low value at pH 7 (Fig. 1a).

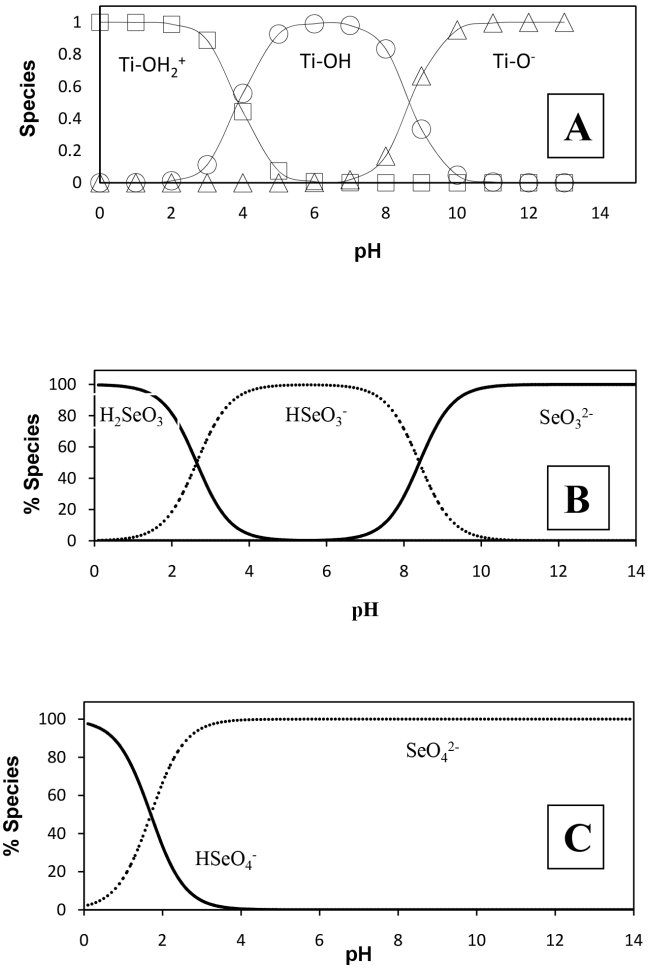

Fig. 1. A–C: Speciation diagrams as a function of pH: A) TiO_2 speciation; B) Se(IV) speciation; C) Se(VI) speciation (Calculated using MINTEQ software).

The Se(IV) adsorption (Fig. 2a) also shows a similar decreasing trend. Shi et al. [24] also report decreasing Se(IV) adsorption onto TiO_2 with an increase in pH. Now adding 5 ppm Se(VI) to the respective single Se(IV)-only system does not cause any significant change in Se(IV) adsorption and similar is noted for 10 ppm Se(VI) (Fig. 2a). This fact was supported by results from additional adsorption studies completed at 5 ppm Se(IV) (Fig. 2b) that also show that an increase in Se(VI) from 5 to 10 ppm has no significant effect onto Se(IV) adsorption. This indicates that relative affinity of TiO_2 is higher for Se(IV) compared to Se(VI) species. This might result because of differences in the type of surface complexes that Se(IV) and Se(VI) species form with the TiO_2 surface sites. Balistrieri and Chao [49] who studied the adsorption of selenium species onto amorphous iron oxyhydroxide and manganese dioxide also observed higher surface affinity for Se(IV) relative to Se(VI). Hence the displacement of surface bound Se(IV) by the aqueous

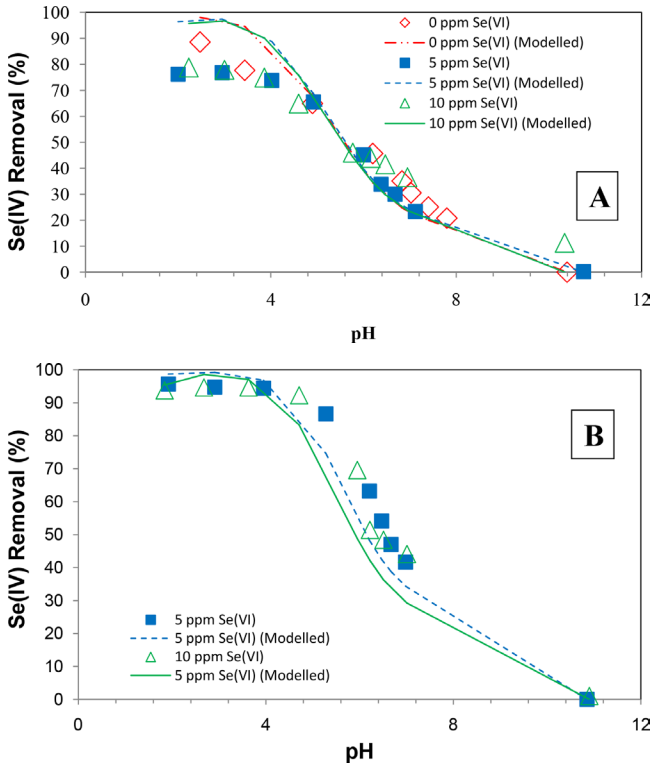

Fig. 2. A-B: Experimental and modelling results for Se(IV) adsorption onto (1 g/L) TiO_2 in presence of Se(VI): A) 10 ppm Se(IV); B) 5 ppm Se(IV).

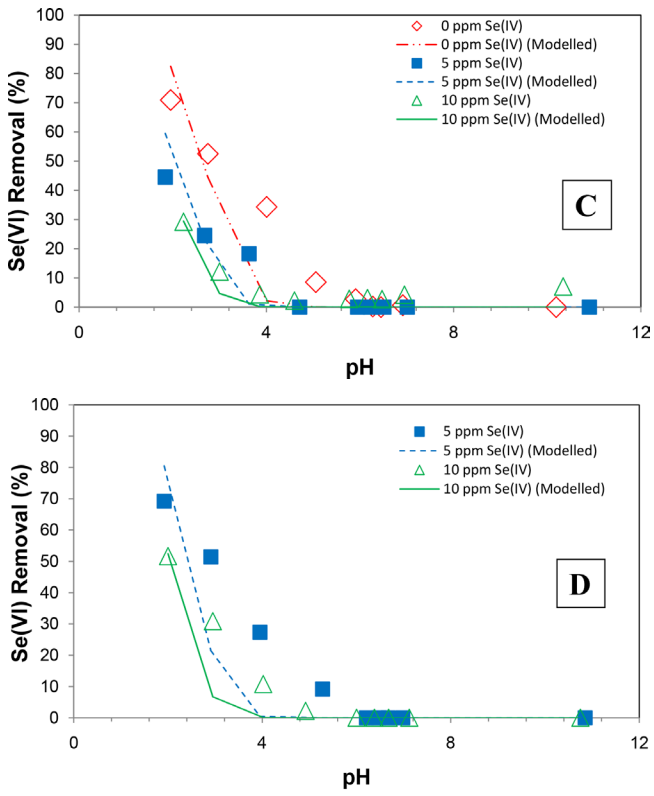

Fig. 2. C-D: Experimental and modelling results for Se(VI) adsorption onto (1 g/L) TiO_2 in presence of Se(IV): C) 10 ppm Se(VI); D) 5 ppm Se(VI).

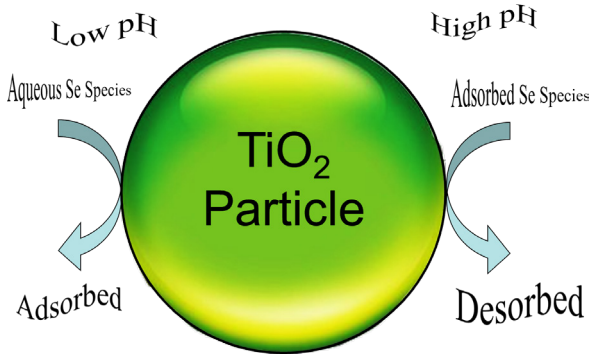

Scheme 1: A qualitative depiction of adsorption of selenium species on to TiO_2 as function of pH.

Se(VI) species will be difficult. Vohra [19] who studied TiO_2 assisted photocatalysis of $SeCN^-$ species also noted albeit slower Se(VI) buildup from oxidation of surface bound Se(IV) species; the resulting Se(VI) species then diffused into bulk aqueous phase as a result of solid-solution equilibrium and also because of comparatively lower Se(VI) affinity for the TiO_2 surface. Tan et al. [38] and Nguyen et al. [34,35], who report brief Se(IV)/Se(VI) adsorption onto TiO_2 also report somewhat higher Se(IV) adsorption onto TiO_2 compared to Se(VI) species. The authors suggest that different surface complexation mechanisms because of different Se(IV)/Se(VI) molecular structures could explain the respective differences in the adsorption trends.

Also comparing the results from Figs. 2a and 2b, a higher percent-based Se(IV) adsorption is noted for the 5 ppm Se(IV) systems as compared to the 10 ppm Se(IV) systems (Figs. 2b and 2a, respectively). For example approx. 96%, 94%, and 54%, Se(IV) adsorption is achieved for the 5 ppm Se(IV)/5 ppm Se(VI) system at pH 2, 4, and 7 respectively (Fig. 2b), whereas for the 10 ppm Se(IV)/5 ppm Se(VI), Se(IV) adsorption is 76%, 74%, and 34%, at pH 2, 4, and 7, respectively (Fig. 2a). The decrease in percent-based Se(IV) adsorption with an increase in its concentration might be as a result of saturation of the limited TiO_2 surface sites. However it should be noted that on mass basis the adsorption values are still higher for the 10 ppm Se(IV) system because of corresponding higher mass transfer driving force across the bulk aqueous and bulk solid phase.

The *Diffuse Layer Model* (DLM) was also employed for the adsorption modelling of above mentioned experimental findings. In that regard several surface-binding possibilities (for Se(IV) and Se(VI)) were considered and eventually those surface complexes that yielded the best match for most (if not all) experimental adsorption matrices including the tertiary systems (as discussed later) were adopted for the modelling purpose. Table 2 provides the respective surface complexation details whereas Table 3 provides some of aqueous speciation reactions.

For the 10 ppm Se(IV) systems, a good correlation between the experimental results and model estimates is typically noted (Fig. 2a) except at pH 2 and 3 where the model overestimates Se(IV) adsorption. A similar trend is observed for the 5 ppm Se(IV) systems (Fig. 2b), albeit with good correlation at all pH values. In general the model delivers better adsorption estimates under a varying set of

conditions including pH and Se(IV)/Se(VI) concentrations. Modelling output details show that for Se(IV), consideration of Ti-SeO_3^-surface complex provides a good model fit, whereas in case of Se(VI) (discussed in detail in the coming section) the Ti-H_2O-SeO_4^- is noted to provide better model fits. Also the formation of both inner sphere and outer sphere type surface complexation has been noted for TiO_2. In case of anion forming an inner sphere complex, results in Ti-Anion complex with the displacement of surface OH group. However in case of an outer sphere complex, the adsorbing species interacts via surface H_2O group. In any case all such interactions are predominantly electrostatic in nature. Also surface complexation reactions as given in Table 2 consider both ion and charge number, and the DLM model automatically considers any changes in aqueous speciation (for all species) and surface species w.r.t. pH, and eventually those changes are also incorporated into the adsorption modelling results.

For Se(IV) species adsorption, several studies have indicated the formation of an inner sphere complex with different surfaces including goethite [54], and TiO_2 [24]. The evidence for such a complexation comes from sources such as no significant effect of ionic strength on adsorption [54–56], and use of advanced analytical techniques including XAS and XPS [56–58]. Hayes et al. [54] employing EXAFS findings indicate formation of an inner sphere complex between Se(IV) and goethite surface, whereas for Se(VI) they report an outer sphere complex formation; the respective analysis for Se(IV) indicated Se-Fe distance of 3.38 Å. Papelis et al. [56,59] report similar observations for Se(IV) adsorption onto aluminum oxide surfaces; Papelis et al. [56] report Se-Al distance of 3.5Å that is supportive of an inner sphere complex. Also Gurkan et al. [60] who investigated Se(IV)-doped TiO_2 synthesis noted increased Ti- and O- species binding energies (based on XPS data) and attributed it to Ti-O-Se bond formation; the Se species in the bond was noted to be Se(IV) as well. In the present study an XPS analysis was also completed for TiO_2 samples after the adsorption of respective selenium anions and the results that are presented in Fig. 3 show that for Se(IV) and Se(VI) adsorbed TiO_2 samples, O 1s and Ti 2p3/2 binding energies are about 530 eV and 458.5 eV respectively. This shows that TiO_2 exist in +4 state as Ti^{4+} respective samples. By fixing the main C 1s binding energy at 248.8 eV, Se 3p3/2 binding energies for Se(IV) and Se(VI) containing samples are found to be 165.6 and 166.2 respectively. The relative difference in the energy level between the TiO_2 samples containing Se(IV) and Se(VI) was found to be 0.6 eV. Sartz et al. [61] who inves-

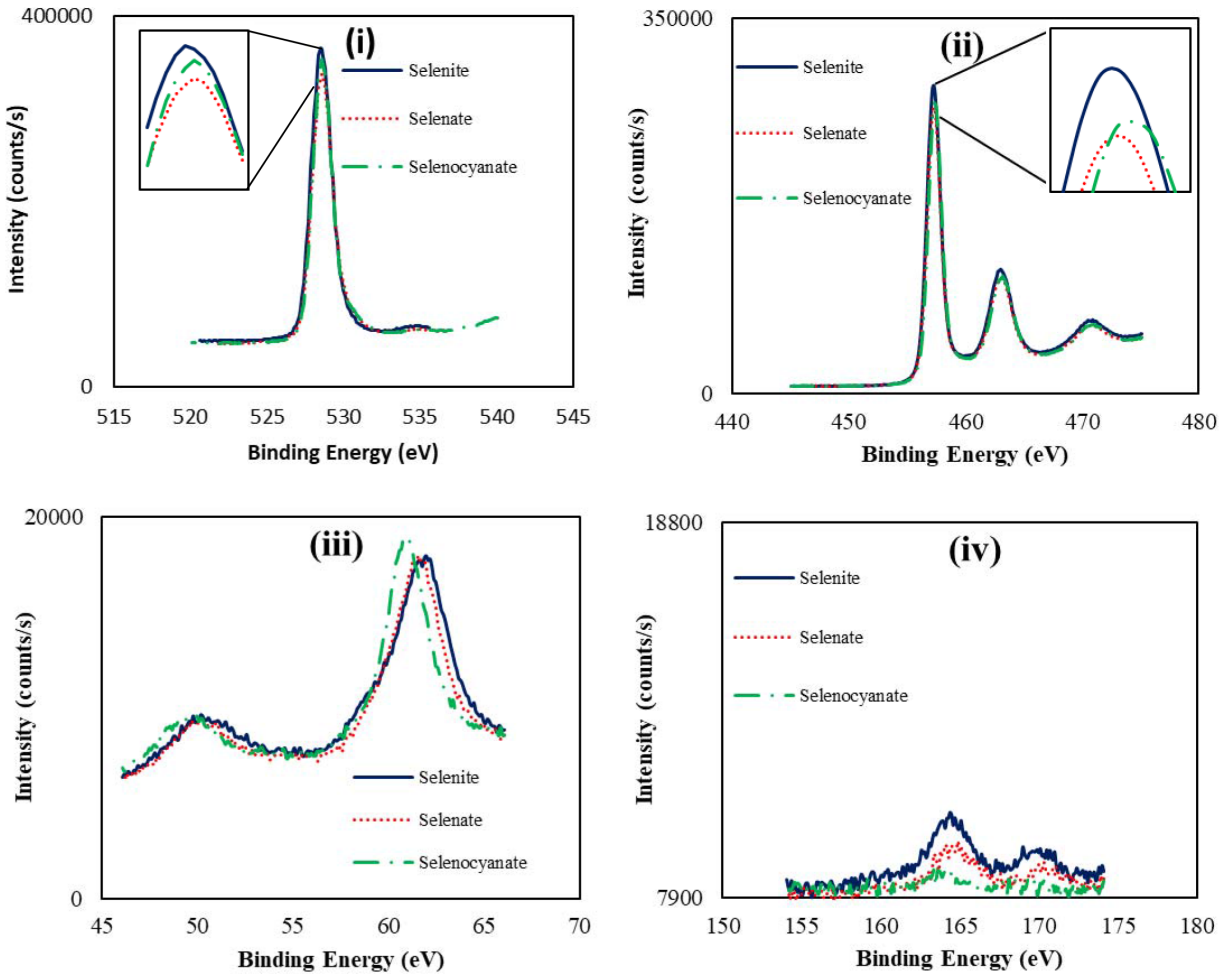

Fig. 3. X-ray photoelectron spectroscopy (XPS) spectra of TiO_2 samples for the adsorption of Se(IV), Se(VI) and $SeCN^-$ (i) O 1s, (ii) Ti 2p, (iii) Se 3d, (iv) Se 3p.

tigated selenium species XPS spectra obtained Se 3p3/2 binding energies of 164.6, 164.1 and 159.1 eV for selenium in +6, +4 and –2 oxidation states and difference in binding energies between +6 and +4 oxidation state species is about 0.5 eV. The similarity (between the present study and above mentioned study) regarding the relative difference in the binding energies for Se(IV) and Se(VI) indicates that Se(IV) and Se(VI) are adsorbed on the TiO_2 surface reaching a thermodynamically stable state [62].

Furthermore the Se(VI) adsorption results from above discussed systems are also summarized here. Fig. 2c shows the adsorption findings for 10 ppm Se(VI) in the presence of 0 to 10 ppm Se(IV). For the 10 ppm Se(VI) system without Se(IV) (Fig. 2c), about 71, 52, 34, and 9% Se(VI) adsorption transpires at equilibrium pH of 2, 3, 4 and 5, respectively. A sharp decrease in Se(VI) adsorption is observed with an increase in pH from 2 to 5, with insignificant adsorption observed above pH 5. Se(VI) speciation (Fig. 1c) shows that near pH 1.7, about 50% of Se(VI) is in the form of $HSeO_4^-$, which reduces to negligible amount at pH 4 and above. Likewise, TiO_2 speciation (Fig. 1a) also shows declining cationic $TiOH_2^+$ species above pH 4. Therefore, since both anionic $HSeO_4^-$ and cationic $TiOH_2^+$ species decrease with an increase in pH, the electrostatic attraction between the two species also decrease with an increase in pH thus resulting into reduced Se(VI) adsorption.

Addition of 5 ppm Se(IV) to 10 ppm Se(VI) system (Fig. 2c) results into decreased Se(VI) adsorption, i.e., 45, 25, 18, and 0% at pH 2, 3, 4 and 5, respectively. Furthermore at 10 ppm Se(IV), Se(VI) adsorption decreases further (Fig. 2c). For example the respective Se(VI) adsorption values at pH 2 are as follows: 71% at 0 ppm Se(IV), 45% at 5 ppm Se(IV), and 29% at 10 ppm Se(IV). Results from 5 ppm Se(VI) (Fig. 2d) show similar trends, i.e., an increase in Se(IV) from 5 to 10 ppm also decreases Se(VI) adsorption from 69, 51, 27, and 9% to 52, 31, 11, and 2% at pH 2, 3, 4, and 5, respectively. Decrease in Se(VI) adsorption with increase in Se(IV) concentration can be attributed to: 1) higher affinity of Se(IV) to the TiO_2 surface compared to Se(VI), and 2) difference in the type of surface complex they formed with the TiO_2 surface. XPS results explained earlier shows that Se(VI) is adsorbed via the formation of outer-sphere complex while Se(IV) is adsorbed via the formation of stronger inner-sphere complex. Tan et al. [38] also observed a decrease in Se(VI) adsorption when formate was introduced to the system.

In any case these findings indicate the differences in Se(IV) and Se(VI) interactions with the metal oxide surfaces. Also the Se(VI) adsorption results (Figs. 2c and 2d) show lower removals compared to respective Se(IV) adsorption results (Figs. 2a and 2b). These findings also indicate preferential Se(IV) adsorption on to TiO_2 surface. Comparing results in Figs. 2c and 2d, a decrease in percent Se(VI) adsorption is also observed when its initial concentration is increased from 5 to 10 ppm. Nevertheless Se(VI) removal on mass basis is still higher for 10 ppm Se(VI). Fig. 2c also shows that the *Diffuse Layer Model* reasonably predicts Se(VI) adsorption whereas trends in Fig. 2d show some underestimations. Also both the experimental and modelling results show adsorption transpiring between a narrow pH range of 2–5 (Figs. 2c–d).

To build on above given Se(IV)/Se(VI) adsorption findings, studies on adsorption of Se(IV)/$SeCN^-$ binary systems (Figs. 4a–d) were also completed. However, unlike the above mentioned Se(IV)/Se(VI) systems, a pinkish precipitate formation was noticed during $SeCN^-$ adsorption work. To ascertain the source of the precipitation, two blank $SeCN^-$ experiments were completed without TiO_2 and the results are presented in Fig. 5. About 99%, 66%, 17% and 15% selenium precipitation was observed for 10 ppm $SeCN^-$ at pH 2, 3, 4 and 5 respectively whereas 77% and 24% selenium precipitation was observed at pH 2 and 3 for the 5 ppm $SeCN^-$, respectively. The precipitation resulted from the breakdown of $SeCN^-$ complex according to Eq. (1) as suggested by Hamada [63]:

$$SeCN^- + H^+ \rightarrow HCN + Se^0 \quad (1)$$

Hence the precipitation results in Fig. 5 were duly deducted from the respective overall $SeCN^-$ removal before modelling the adsorption of $SeCN^-$ using Ti-H_2O-SeCN type surface complex. Similar to Se(IV)/Se(VI) systems (Fig. 2) $SeCN^-$ also shows no significant effect onto Se(IV) adsorption (Figs. 4a–b) that can be explained based on aforementioned discussion on an inner-sphere type Se(IV) complexation. However unlike the suppresive effect of Se(IV) onto Se(VI) removal (Figs. 2c–d), no notable effect of Se(IV) onto $SeCN^-$ removal is observed and the respective $SeCN^-$ removal trend lines are somewhat more gradual in their drop from acidic to basic pH range (Figs. 4c–d) as compared to Se(VI) (in Se(IV)/Se(VI) systems) that showed a sharp adsorption edge transpiring between a narrow pH range of 2 till 5 (Figs. 2c–d). Also, the respective $SeCN^-$ removal results above pH 4 are higher in comparison to Se(VI) removal. Hence the $SeCN^-$ removal findings from Se(IV)/$SeCN^-$ binary systems (Figs. 4c–d) are somewhat different from Se(VI) removal from Se(IV)/Se(VI) binary systems (Figs. 2c–d). In general for the binary Se(IV)/$SeCN^-$ systems, high Se(IV) removals can be achieved with insignificant $SeCN^-$ effect. The respective $SeCN^-$ modelling results as provided in Fig. 4 also show a good match between the experimental and modelling results using an outer sphere type complex. Nevertheless if $SeCN^-$ also forms an outer sphere type complex then question arises why its removal is not affected by Se(IV) (Figs. 4c–d) unlike the Se(VI) species removal (Figs. 2c–d). This query lead us to conduct another set of experiments for Se(VI) and $SeCN^-$ mixed systems. Results for binary Se(VI)/$SeCN^-$ adsorption results are provided in Figs. 6a–d. No notable effect of $SeCN^-$ onto Se(VI) removal (Figs. 6a–b) was noted, which is qualitatively similar to Se(IV) trends in Se(IV)/$SeCN^-$ systems (Figs. 4a–b). Also similar to Se(IV)/$SeCN^-$ results (Figs. 4c–d), no notable Se(VI) effect is observed on $SeCN^-$ removal (Figs. 6c–d). In any case the above results indicate adsorption trends that are important to understand any respective treatment applications. The current work was further extended for tertiary systems and the respective results are given below.

3.2. Tertiary systems

After completing the above mentioned binary-systems adsorption studies, the present work was extended to investigate Se(IV), Se(VI) and $SeCN^-$ adsorption trends under several tertiary system conditions. In that regard, the adsorption of respective selenium species onto TiO_2 was

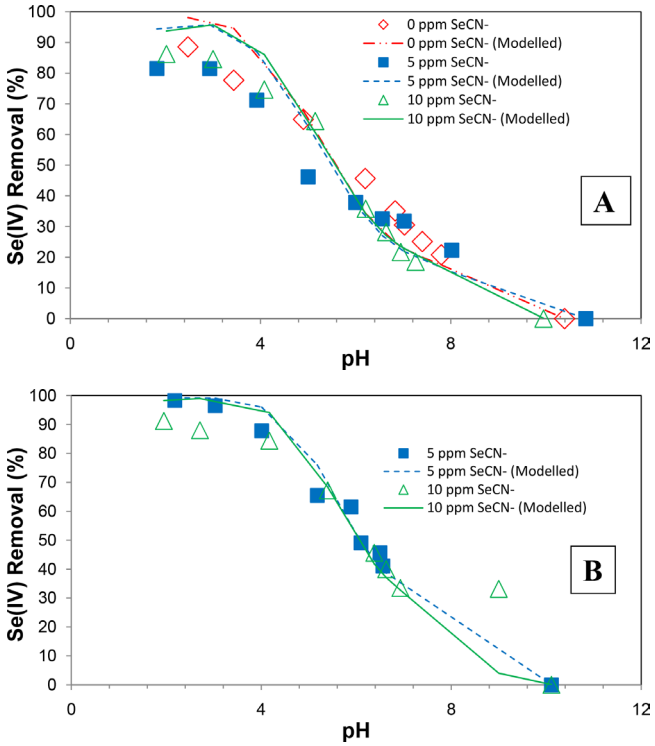

Fig. 4. A-B: Experimental and modelling results for Se(IV) adsorption onto (1 g/L) TiO_2 in presence of $SeCN^-$: A) 10 ppm Se(IV); B) 5 ppm Se(IV).

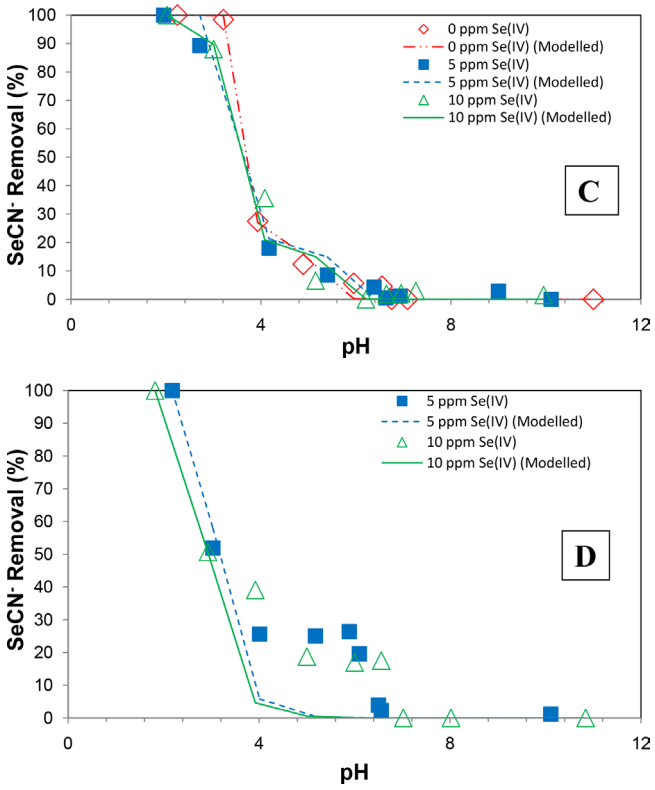

Fig. 4. C-D: Experimental and modelling results for $SeCN^-$ adsorption onto (1 g/L) TiO_2 in presence of Se(IV): C) 10 ppm $SeCN^-$; D) 5 ppm $SeCN^-$.

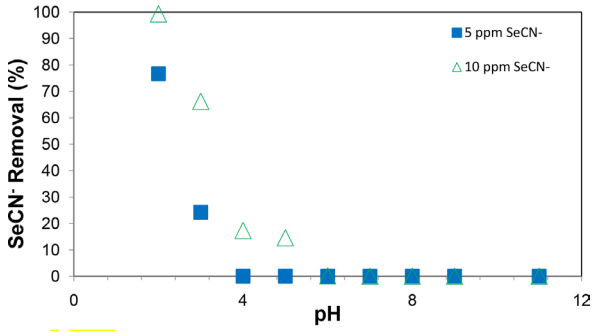

Fig. 5. $SeCN^-$ precipitation trends in the absence of TiO_2.

studied at varying pH values and tertiary solution matrices. The respective experimental and modelling results are given below.

The results for the effect of Se(VI) onto 10 ppm Se(IV) adsorption in the presence of 5 ppm $SeCN^-$ are shown in Fig. 7a. In the absence of Se(VI), about 82%, 71%, 33% and 0% adsorption values (Fig. 7a) are observed at pH 2, 4, 7 and 11, respectively. An introduction of 5 ppm Se(VI) concentration to the above system shows no significant change in Se(IV) removal. Also an increase in Se(VI) concentration from 5 ppm to 10 ppm shows a similar trend.

The effect of Se(VI) concentration was further investigated on the adsorption of 5 ppm Se(IV) in tertiary system containing 5 ppm $SeCN^-$ (Fig. 7b), that also shows no significant change. Furthermore, the findings in Fig. 7c for 10 ppm Se(IV) and 10 ppm $SeCN^-$ though show that an increase in Se(VI) concentration (from 0 to 10 ppm) leads to some decrease in Se(IV) adsorption specifically at low pH values (e.g., at pH 2, 86%, 69%, and 64% Se(IV) adsorption was achieved for the 0 ppm, 5 ppm, and 10 ppm Se(VI) systems respectively), the results above pH 4 show no Se(VI) effect onto Se(IV) removal (Fig. 7c). Also similar to the single and binary systems, a gradual decrease in Se(IV) adsorption for pH 2 to 4, is followed by sharp change between pH 4 and 7. Furthermore, Figs. 7a–d show that a good correlation exists between the model predicted values and experimental results, except for the tertiary systems in Fig. 7c (5 ppm Se(VI)/10 ppm Se(IV)/10 ppm $SeCN^-$ and 10 ppm Se(VI)/10 ppm Se(IV)/10 ppm $SeCN^-$) where the model overestimates the adsorption at low pH values. In general, Se(VI) effect onto Se(IV) removal in presence of $SeCN^-$ (Fig. 7) is not significant.

Similar to the binary systems, higher percent Se(IV) adsorption was also observed for tertiary system with 5 ppm Se(IV) concentration (Figs. 7b and 6d) as compared to 10 ppm Se(IV) concentration (Figs. 7a and 7c). Nevertheless adsorption on mass basis is still higher for 10 ppm Se(IV) systems due to higher mass transfer driving force across the thin film between the bulk aqueous and bulk solid phase. Regarding the effect of $SeCN^-$ on the adsorption of Se(IV) from above discussed tertiary systems, some decrease in Se(IV) adsorption was noted especially at acidic pH and 10 ppm $SeCN^-$ (Figs. 8a–d). Nevertheless such differences tend to reduce at pH above 4 and trends look to be similar to respective binary system results (Figs. 4a–b).

Now looking into the effect of Se(IV) species onto Se(VI) adsorption as summarized in Fig. 9, about 68, 44, 38, and 16%

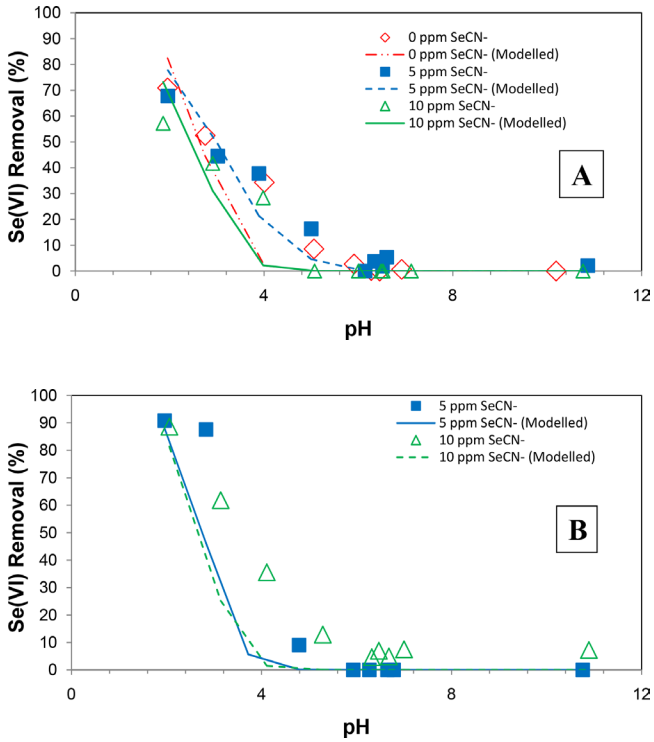

Fig. 6. A-B: Experimental and modelling results for Se(VI) adsorption onto (1 g/L) TiO_2 in presence of $SeCN^-$: A) 10 ppm Se(VI); B) 5 ppm Se(VI).

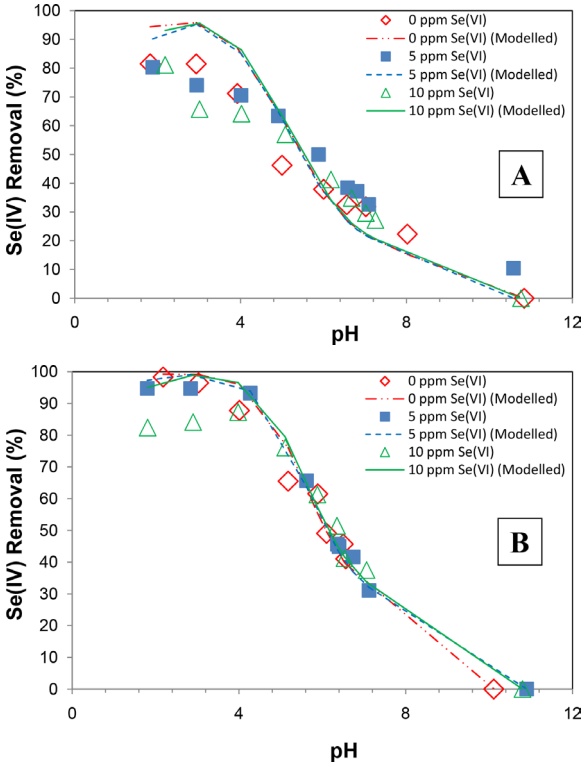

Fig. 7. A-B: Experimental and modelling results for Se(IV) adsorption onto (1 g/L) TiO_2 in presence of Se(VI) and $SeCN^-$: A) 10 ppm Se(IV), 5 ppm $SeCN^-$; B) 5 ppm Se(IV), 5 ppm $SeCN^-$.

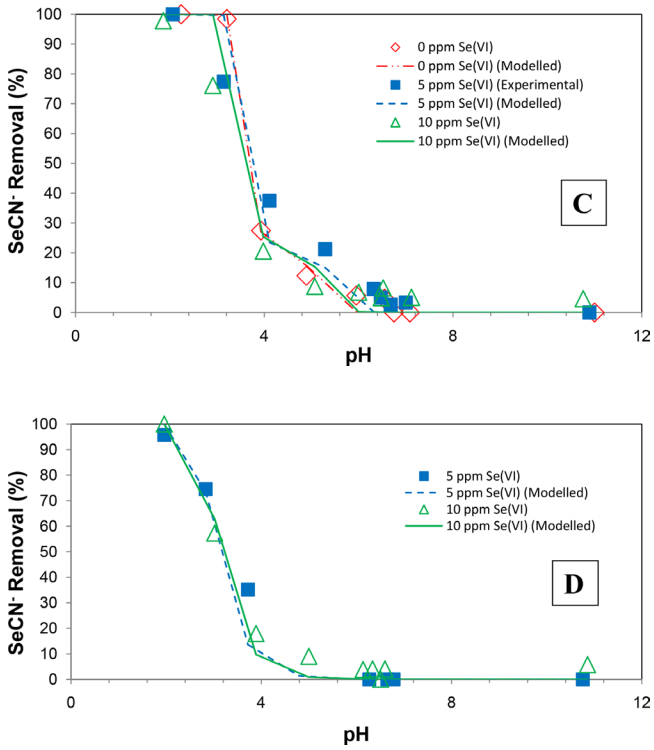

Fig. 6. C-D: Experimental and modelling results for $SeCN^-$ adsorption onto (1 g/L) TiO_2 in presence of Se(VI): C) 10 ppm $SeCN^-$; D) 5 ppm $SeCN^-$.

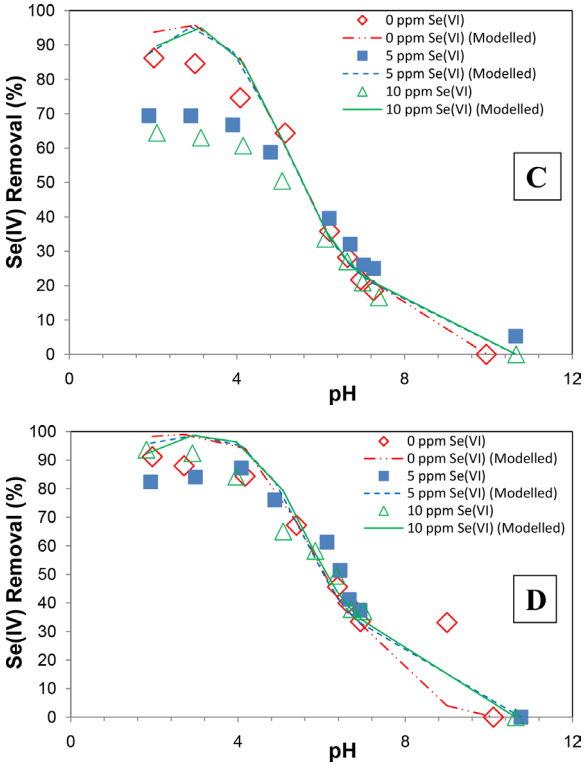

Fig. 7. C-D: Experimental and modelling results for Se(IV) adsorption onto (1 g/L) TiO_2 in presence of Se(VI) and $SeCN^-$: C) 10 ppm Se(IV), 10 ppm $SeCN^-$; D) 5 ppm Se(IV), 10 ppm $SeCN^-$.

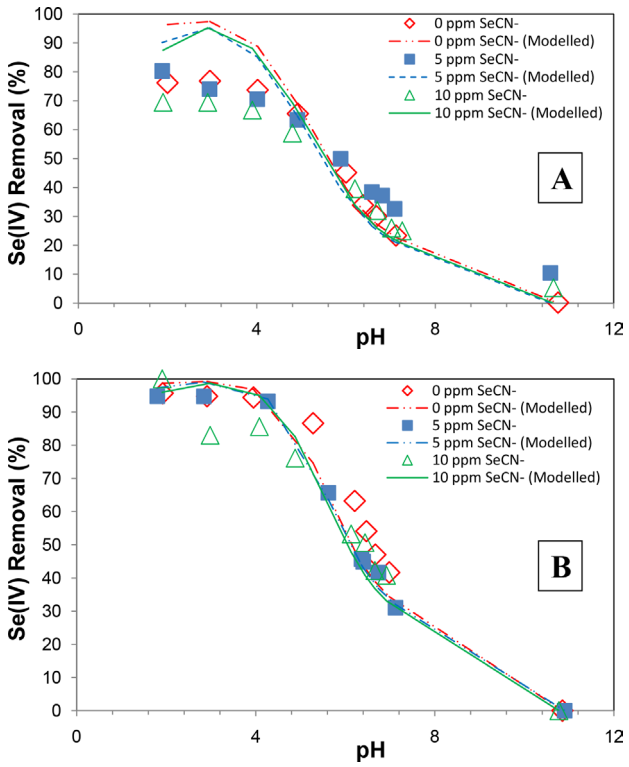

Fig. 8. A-B: Experimental and modelling results for Se(IV) adsorption onto (1 g/L) TiO_2 in presence of Se(VI) and $SeCN^-$: A) 10 ppm Se(IV), 5 ppm Se(VI); B) 5 ppm Se(IV), 5 ppm Se(VI).

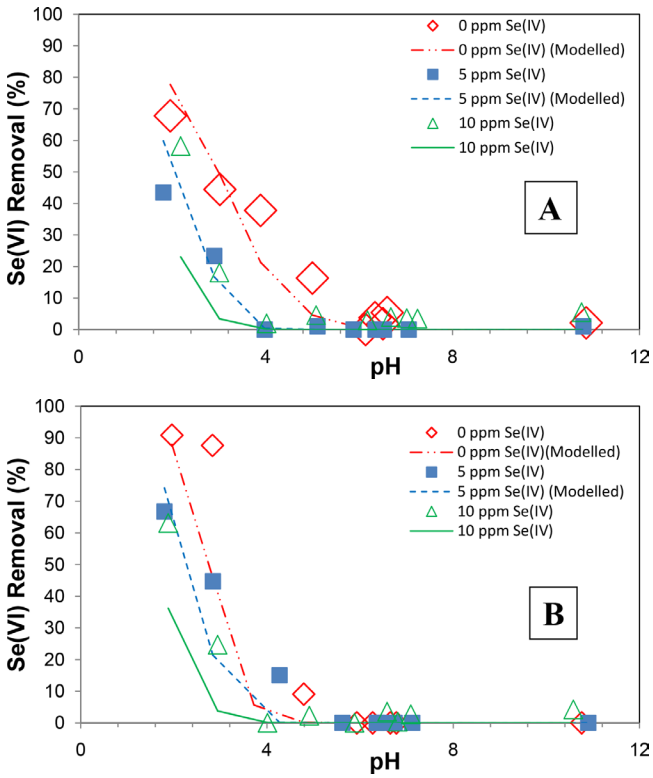

Fig. 9. A-B: Experimental and modelling results for Se(VI) adsorption onto (1 g/L) TiO_2 in presence of Se(IV) and $SeCN^-$: A) 10 ppm Se(VI), 5 ppm $SeCN^-$; B) 5 ppm Se(VI), 5 ppm $SeCN^-$.

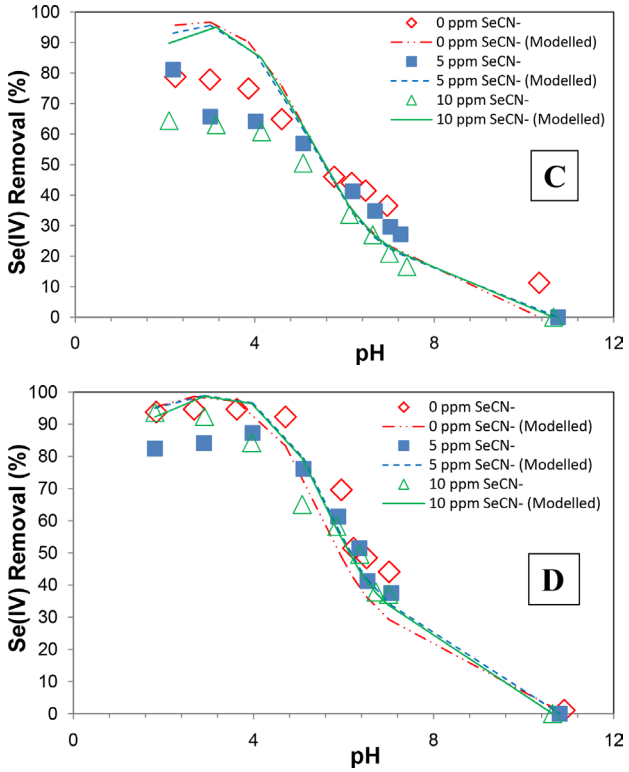

Fig. 8. C-D: Experimental and modelling results for Se(IV) adsorption onto (1 g/L) TiO_2 in presence of Se(VI) and $SeCN^-$: C) 10 ppm Se(IV), 10 ppm Se(VI); D) 5 ppm Se(IV), 10 ppm Se(VI).

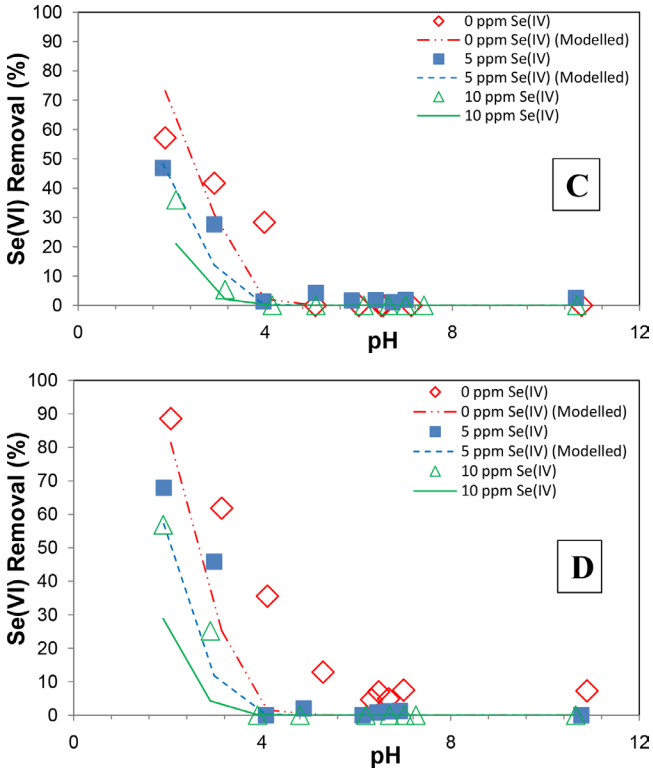

Fig. 9. C-D: Experimental and modelling results for Se(VI) adsorption onto (1 g/L) TiO_2 in presence of Se(IV) and $SeCN^-$: C) 10 ppm Se(VI), 10 ppm $SeCN^-$; D) 5 ppm Se(VI), 10 ppm $SeCN^-$.

Se(VI) adsorption at pH 2, 3, 4 and 5 respectively is noted for 10 ppm Se(VI)/5 ppm $SeCN^-$. As noted for the binary Se(VI)/Se(IV) systems (Figs. 2c and 2d), addition of Se(IV) to the Se(VI)/ $SeCN^-$ system also results into decreased Se(VI) adsorption (Fig. 9a). The effect of Se(IV)onto 5 ppm Se(VI) removal (in the presence of 5 ppm $SeCN^-$) as given in Fig. 9b indicates decreased Se(VI) adsorption of 24%, 43%, and 9% at pH 2, 3 and 5 respectively, compared to 91%, 88%, and 9% Se(VI) adsorption at pH 2, 3 and 5 respectively in the absence of Se(IV). A further increase in Se(IV) concentration from 5 ppm to 10 ppm (Fig. 9b) results in a further decrease in Se(VI) adsorption onto TiO_2. Qualitatively similar *Se(IV)-effect* trends are observed for the adsorption of 10 ppm Se(VI) (Fig. 9c) and 5 ppm Se(VI) (Fig. 9d) in the presence of 10 ppm selenocyante. The adsorption trends in Figs. 9a–d are similar to the binary systems discussed in Figs. 2c and 2d i.e., an increase in both Se(IV) and Se(VI) concentrations causes a decrease in Se(VI)'s overall removal. Also except for the 5 ppm Se(IV)/10 ppm Se(VI)/5 ppm $SeCN^-$ system the model underestimates Se(VI) adsorption (Figs. 9a–d).

The effect of $SeCN^-$ onto Se(VI) adsorption was also investigated for the tertiary systems mentioned in Fig. 9. No significant effect is noted for the 10 ppm Se(VI) and 5 ppm Se(IV) system, i.e., at pH 2, 45%, 44% and 47% Se(VI) adsorption is noted for 0, 5 and 10 ppm $SeCN^-$ concentrations respectively and a qualitatively similar trend is noted for 5 ppm Se(VI). Also the effect of $SeCN^-$ on to Se(VI) adsorption in the presence of 10 ppm Se(IV) shows no significant differences though the overall Se(VI) adsorption is low. These adsorption trends were qualitatively similar to the binary systems discussed in Figs. 6a and 6b that strengthens our earlier comment that Se(VI) adsorption is not affected by the presence of $SeCN^-$. This trend is further supported by the outcomes from the combined effect of Se(IV)/Se(VI) species onto $SeCN^-$ removal that also shows no specific trend. In summary the results and observations presented in this work are very important and aforementioned specific adsorption trends should be carefully considered for an effective treatment of respective selenium species using the TiO_2 based processes under competitive conditions.

4. Conclusions

Competitive adsorption of Se(IV), Se(VI) and $SeCN^-$ species onto TiO_2 was studied under a varying and wide ranging set of conditions and variables, and the respective adsorption results were also successfully modelled using the Diffuse Layer Model. For mixed Se(IV) and Se(VI) binary systems, high Se(IV) adsorption was noted with no noticeable Se(VI) effect onto Se(IV) adsorption even up to 10 ppm Se(VI). However Se(VI) adsorption was markedly affected by the Se(IV) species. This was explained based on higher relative affinity of TiO_2 surface sites for Se(IV) compared to Se(VI) with the former species forming an inner-sphere type complex. Also the Se(IV) adsorption gradually decreased between pH 2 and 4 followed by a sharp decrease till pH 7 whereas for Se(VI) species, a sharp decrease in adsorption was noted from pH 2 to 5. Nevertheless results from the binary Se(IV) and $SeCN^-$ mixed systems indicated no such competitive adsorption trend and similar was also noted for the binary Se(VI) and $SeCN^-$ mixed adsorption studies. Furthermore findings from the tertiary Se(IV), Se(VI), and $SeCN^-$ studies showed similar adsorption trends. In general the adsorption results above pH 4 showed Se(IV) > $SeCN^-$ > Se(VI). For adsorption modelling out of several surface complexation possibilities tested (for wide ranging binary and tertiary mixed conditions) an inner sphere type complex i.e., Ti-SeO_3^- reasonably predicted Se(IV) adsorption whereas Se(VI) and $SeCN^-$ adsorptions were well predicted considering outer sphere complexes, i.e., Ti-H_2O-SeO_4^- and Ti-H_2O-SeCN respectively. Results from the present work indicate that Se(IV), Se(VI), and $SeCN^-$ species can be effectively removed from respective aqueous streams under varying mixed competitive conditions using the TiO_2 based adsorption process with a careful control of process parameters.

Acknowledgement

The authors are thankful to SABIC for providing research grant for this work through project grant SB141004. Also B.A. Labaran is thankful to the King Fahd University of Petroleum and Minerals (KFUPM) for providing support through PhD study program and the submitted work is derived from his PhD thesis [Reference # 53]. Our sincere gratitude to Deanship of Research (KFUPM) for facilitating the grant related matters.

References

[1] D. Wang, G. Alfthan, A. Aro, P. Lahermo, P. Väänänen, The impact of selenium fertilisation on the distribution of selenium in rivers in Finland, Agric. Ecosyst. Environ., 50 (1994) 133–149.
[2] J. Risher, Toxicological profile for selenium, *ATSDR,* 2003.
[3] J. HÖGberg, J.A.N. Alexander, In: M.S. Toprak, H.L. Karlsson, and B. Fadeel, Handbook on the Toxicology of Metals, 3rd Ed., Academic Press, Burlington 2014, pp. 783–807.
[4] P. Zhang, D.L. Sparks, Kinetics of selenate and selenite adsorption/desorption at the goethite/water interface, Environ. Sci. Technol., 24 (1990) 1848–1856.
[5] B. Alley, A. Beebe, J. Rodgers, J.W. Castle, Chemical and physical characterization of produced waters from conventional and unconventional fossil fuel resources, Chemosphere, 85 (2011) 74–82.
[6] M.P. De Souza, I.J. Pickering, M. Walla, N. Terry, Selenium assimilation and volatilization from selenocyanate-treated Indian mustard and muskgrass, Plant Physiol., 128 (2002) 625–633.
[7] N. Aman, T. Mishra, J. Hait, R. Jana, Simultaneous photoreductive removal of copper (II) and selenium (IV) under visible light over spherical binary oxide photocatalyst, J. Hazard. Mater., 186 (2011) 360–366.
[8] N. Bleiman, Y.G. Mishael, Selenium removal from drinking water by adsorption to chitosan–clay composites and oxides: batch and columns tests, J. Hazard. Mater., 183 (2010) 590–595.
[9] N. Geoffroy, G. Demopoulos, The elimination of selenium (IV) from aqueous solution by precipitation with sodium sulfide, J. Hazard. Mater., 185 (2011) 148–154.
[10] X. Hu, F. Wang, M.L. Hanson, Selenium concentration, speciation and behavior in surface waters of the Canadian prairies, Sci. Total Environ., 407 (2009) 5869–5876.
[11] A. Manceau, D.L. Gallup, Removal of selenocyanate in water by precipitation: characterization of copper-selenium precipitate by x-ray diffraction, infrared, and x-ray absorption spectroscopy, Environ. Sci. Technol., 31 (1997) 968–976.
[12] S. Sharmasarkar, G.F. Vance, Selenite–selenate sorption in surface coal mine environment, Adv. Environ. Res., 7 (2002) 87–95.

[13] J. Torres, V. Pintos, L. Gonzatto, S. Dominguez, C. Kremer, E. Kremer, Selenium chemical speciation in natural waters: Protonation and complexation behavior of selenite and selenate in the presence of environmentally relevant cations, Chem. Geol., 288 (2011) 32–38.
[14] N. Zhang, L.-S. Lin, D. Gang, Adsorptive selenite removal from water using iron-coated GAC adsorbents, Water Res., 42 (2008) 3809–3816.
[15] Y. Zhang, C. Amrhein, A. Chang, W.T. Frankenberger, Effect of zero-valent iron and a redox mediator on removal of selenium in agricultural drainage water, Sci. Total Environ., 407 (2008) 89–96.
[16] E. Kikuchi, H. Sakamoto, Kinetics of the reduction reaction of selenate ions by TiO_2 photocatalyst, J. Electrochem. Soc., 147 (2000) 4589–4593.
[17] T.T. Tan, M. Zaw, D. Beydoun, R. Amal, The formation of nano-sized selenium–titanium dioxide composite semiconductors by photocatalysis, J. Nanopart. Res., 4 (2002) 541–552.
[18] B.A. Labaran, M.S. Vohra, Photocatalytic removal of selenite and selenate species: effect of EDTA and other process variables, Environ. Technol., 35 (2014) 1091–1100.
[19] M.S. Vohra, Selenocyanate ($SeCN^-$) contaminated wastewater treatment using TiO_2 photocatalysis: $SeCN^-$ complex destruction, intermediates formation, and removal of selenium species, Fresen. Environ. Bull., 24 (2015) 1108–1118.
[20] M. Kashiwa, S. Nishimoto, K. Takahashi, M. Ike, M. Fujita, Factors affecting soluble selenium removal by a selenate-reducing bacterium Bacillus sp. SF-1, J. Biosci. Bioeng., 89 (2000) 528–533.
[21] G. Banuelos, G. Cardon, B. Mackey, J. Ben-Asher, L. Wu, P. Beuselinck, S. Akohoue, S. Zambrzuski, Boron and selenium removal in boron-laden soils by four sprinkler irrigated plant species, J. Environ. Qual., 22 (1993) 786–792.
[22] V. Mavrov, S. Stamenov, E. Todorova, H. Chmiel, T. Erwe, New hybrid electrocoagulation membrane process for removing selenium from industrial wastewater, Desalination, 201 (2006) 290–296.
[23] A.P. Murphy, Removal of selenate from water by chemical reduction, Ind. Eng. Chem. Res., 27 (1988) 187–191.
[24] K. Shi, X. Wang, Z. Guo, S. Wang, W. Wu, Se (IV) sorption on TiO_2: Sorption kinetics and surface complexation modeling, Colloid Surface A, 349 (2009) 90–95.
[25] K. Foo, B. Hameed, Insights into the modeling of adsorption isotherm systems, Chem. Eng. J., 156 (2010) 2–10.
[26] Y.-S. Ho, Review of second-order models for adsorption systems, J. Hazard. Mater., 136 (2006) 681–689.
[27] H. Qiu, L. Lv, B.-c. Pan, Q.-j. Zhang, W.-m. Zhang, Q.-x. Zhang, Critical review in adsorption kinetic models, J. Zhejiang Univ-Sci. A, 10 (2009) 716–724.
[28] R. Schmuhl, K. Keizer, A. van den Berg, E. Johan, D.H. Blank, Controlling the transport of cations through permselective mesoporous alumina layers by manipulation of electric field and ionic strength, J. Colloid Interface Sci., 273 (2004) 331–338.
[29] N.P. Cheremisinoff, P.N. Cheremisinoff, Carbon adsorption for pollution control, PTR Prentice Hall, New York, USA 1993.
[30] C. Su, D.L. Suarez, Selenate and selenite sorption on iron oxides an infrared and electrophoretic study, Soil Sci. Soc. Am. J., 64 (2000) 101–111.
[31] U. Saha, C. Liu, L. Kozak, P. Huang, Kinetics of selenite adsorption on hydroxyaluminum-and hydroxyaluminosilicate-montmorillonite complexes, Soil Sci. Soc. Am. J., 68 (2004) 1197–1209.
[32] J.S. Yamani, A.W. Lounsbury, J.B. Zimmerman, Adsorption of selenite and selenate by nanocrystalline aluminum oxide, neat and impregnated in chitosan beads, Water Res., 50 (2014) 373–381.
[33] S. Li, N. Deng, Separation and preconcentration of Se (IV)/Se (VI) species by selective adsorption onto nanometer-sized titanium dioxide and determination by graphite furnace atomic absorption spectrometry, Anal. Bioanal. Chem., 374 (2002) 1341–1345.
[34] V.N.H. Nguyen, D. Beydoun, R. Amal, Photocatalytic reduction of selenite and selenate using TiO_2 photocatalyst, J. Photochem. Photobiol. A, 171 (2005) 113–120.
[35] V.N.H. Nguyen, R. Amal, D. Beydoun, Photocatalytic reduction of selenium ions using different TiO_2 photocatalysts, Chem. Eng. Sci., 60 (2005) 5759–5769.
[36] S. Sanuki, K. Arai, T. Kojima, S. Nagaoka, H. Majima, Photocatalytic reduction of selenate and selenite solutions using TiO_2 powders, Metall. Mater. Trans. B., 30 (1999) 15–20.
[37] S. Sanuki, K. Shako, S. Nagaoka, H. Majima, Photocatalytic reduction of Se ions using suspended anatase powders, Mater. Trans. JIM, 41 (2000) 799–805.
[38] T. Tan, D. Beydoun, R. Amal, Effects of organic hole scavengers on the photocatalytic reduction of selenium anions, J. Photochem. Photobiol. A, 159 (2003) 273–280.
[39] T.T.Y. Tan, C.K. Yip, D. Beydoun, R. Amal, Effects of nano-Ag particles loading on TiO_2 photocatalytic reduction of selenate ions, Chem. Eng. J., 95 (2003) 179–186.
[40] T.T. Tan, D. Beydoun, R. Amal, Photocatalytic reduction of Se (VI) in aqueous solutions in UV/TiO_2 system: importance of optimum ratio of reactants on TiO_2 surface, J. Mol. Catal. A, 202 (2003) 73–85.
[41] T.T. Tan, D. Beydoun, R. Amal, Photocatalytic reduction of Se (VI) in aqueous solutions in UV/TiO_2 system: kinetic modeling and reaction mechanism, J. Phys. Chem. B, 107 (2003) 4296–4303.
[42] G. Liu, J. Zhao, Photocatalytic degradation of dye sulforhodamine B: a comparative study of photocatalysis with photosensitization, New J. Chem., 24 (2000) 411–417.
[43] S. Pelet, J.-E. Moser, M. Grätzel, Cooperative effect of adsorbed cations and iodide on the interception of back electron transfer in the dye sensitization of nanocrystalline TiO_2, J. Phys. Chem. B, 104 (2000) 1791–1795.
[44] Y. Xu, C.H. Langford, UV- or visible-light-induced degradation of X3B on TiO_2 nanoparticles: the influence of adsorption, Langmuir, 17 (2001) 897–902.
[45] J. Zhao, T. Wu, K. Wu, K. Oikawa, H. Hidaka, N. Serpone, Photoassisted degradation of dye pollutants. 3. Degradation of the cationic dye rhodamine B in aqueous anionic surfactant/TiO_2 dispersions under visible light irradiation: evidence for the need of substrate adsorption on TiO_2 particles, Environ. Sci. Technol., 32 (1998) 2394–2400.
[46] F. Hingston, A. Posner, J. Quirk, Competitive adsorption of negatively charged ligands on oxide surfaces, Discuss. Faraday Soc., 52 (1971) 334–342.
[47] K.-H. Goh, T.-T. Lim, Geochemistry of inorganic arsenic and selenium in a tropical soil: effect of reaction time, pH, and competitive anions on arsenic and selenium adsorption, Chemosphere, 55 (2004) 849–859.
[48] C.-H. Wu, S.-L. Lo, C.-F. Lin, Competitive adsorption of molybdate, chromate, sulfate, selenate, and selenite on γ-Al_2O_3, Colloid Surface A, 166 (2000) 251–259.
[49] L.S. Balistrieri, T. Chao, Adsorption of selenium by amorphous iron oxyhydroxide and manganese dioxide, Geochim. Cosmochim. Acta, 54 (1990) 739–751.
[50] L.S. Balistrieri, T.T. Chao, Selenium adsorption by Goethite1, Soil Sci. Soc. Am. J., 51 (1987) 1145–1151.
[51] K.F. Hayes, G. Redden, W. Ela, J.O. Leckie, Surface complexation models: an evaluation of model parameter estimation using FITEQL and oxide mineral titration data, J. Colloid Interface Sci., 142 (1991) 448–469.
[52] M.S. Vohra, A.P. Davis, Adsorption of Pb (II), EDTA, and Pb (II)-EDTA onto TiO_2, J. Colloid Interface Sci., 198 (1998) 18–26.
[53] B.A. Labaran, Competitive Photocatalytic Removal of Aqueous Phase Selenocyanate ($SeCN^-$) in the Presence of Some Critical Co-pollutants: Adsorption Modelling, Process Kinetics, and Reaction Mechanisms, (*Thesis, PhD*) King Fahd University of Petroleum and Minerals, Dhahran, Kingdom of Saudi Arabia, May 2017.
[54] K.F. Hayes, A.L. Roe, G.E. Brown Jr, K.O. Hodgson, J.O. Leckie, G.A. Parks, In situ X-ray absorption study of surface complexes: selenium oxyanions on α-FeOOH, Science, 238 (1987) 783–786.
[55] P.V. Brady, The physics and chemistry of mineral surfaces, CRC Press 1996.

[56] C. Papelis, G.E. Brown Jr, G.A. Parks, J.O. Leckie, X-ray absorption spectroscopic studies of cadmium and selenite adsorption on aluminum oxides, Langmuir, 11 (1995) 2041–2048.
[57] E.J. Boyle-Wight, L.E. Katz, K.F. Hayes, Macroscopic studies of the effects of selenate and selenite on cobalt sorption to γ-Al_2O_3, Environ. Sci. Technol., 36 (2002) 1212–1218.
[58] J. Huang, Z. Wu, L. Chen, Y. Sun, Surface complexation modeling of adsorption of Cd (II) on graphene oxides, J. Mol. Liq., 209 (2015) 753–758.
[59] C. Papelis, P.V. Roberts, J.O. Leckie, Modeling the rate of cadmium and selenite adsorption on micro-and mesoporous transition aluminas, Environ. Sci. Technol., 29 (1995) 1099–1108.
[60] Y.Y. Gurkan, E. Kasapbasi, Z. Cinar, Enhanced solar photocatalytic activity of TiO_2 by selenium (IV) ion-doping: characterization and DFT modeling of the surface, Chem. Eng. J., 214 (2013) 34–44.
[61] W.E. Sartz Jr, K.J. Wynne, D.M. Hercules, X-ray photoelectron spectroscopic investigation of Group VIA elements, Anal. Chem., 43 (1971) 1884–1887.
[62] K.S. Smith, Metal sorption on mineral surfaces: an overview with examples relating to mineral deposits, Environ. Geochem. Miner. Depos. B, 6 (1999) 161–182.
[63] S. Hamada, Acid decomposition equilibrium of selenocyanate ion, Nippon Kagaku Zasshi, 82 (1961) 1327–1330.